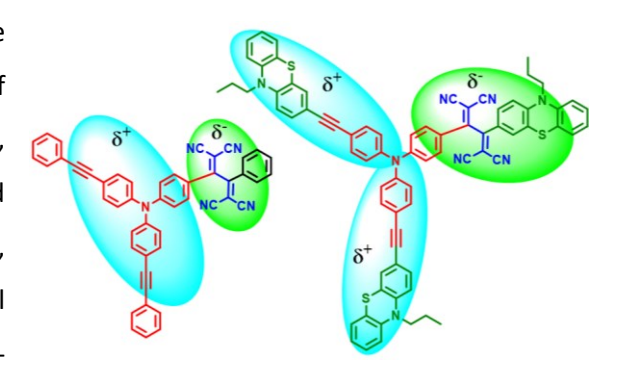
Star-Shaped Triphenylamine-Tetracyanobutadiene-Phenothiazine Push-Pull Systems: Role of Terminal Phenothiazine in Improving Charge Transfer

Indresh Singh Yadav a,‡ Ajyal Z. Alsaleh b,‡ Rajneesh Misraa,* and Francis D'Souza,b*

^aDepartment of Chemistry, Indian Institute of Technology, Indore 453552, India

^bDepartment of Chemistry, University of North Texas, 1155 Union Circle, #305070, Denton, TX 76203-5017, USA

Abstract: Understanding the process of charge transfer in multi-modular push-pull systems is of great significance for technology breakthroughs, especially in the areas of light energy conversion and building optoelectronic devices. In the present study, a series of symmetrical and unsymmetrical push-pull systems, **1–4** were designed and synthesized via Pd-



catalyzed Sonogashira cross-coupling reaction, followed by [2+2] cycloaddition-retroelectrocyclization reaction. The D- π -D₃' and D-A_n-D₃' (n = 0-3) molecular configurations of **1–4** contained triphenylamine (TPA), D as the central core, and phenothiazine (PTZ), D' as the end-capping unit as a donor and TCBD as the central electron acceptor, A. As control compounds, **C1–C4** with a general formula, D-A_n were also synthesized to realize the effect of terminal PTZ in the charge transfer events. The photophysical properties of both star-shaped symmetrical and unsymmetrical **2–4** molecules exhibited a broad intramolecular charge transfer (ICT, also known as charge polarization) band in the visible-near IR region due to strong push-pull interactions. The electrochemical properties of both the **1–4** and **C1–C4** series exhibited multistep redox processes, and spectroelectrochemical studies helped in arriving at the spectral features of the charge transfer species. Frontier orbitals generated on DFT optimized structures helped in visualizing the charge transfer within the different donor and acceptor entities of a given push-pull system. Finally, femtosecond transient absorption spectral studies followed by data analysis by target analyses were utilized to demonstrate excited charge transfer. The terminal PTZ in compounds **2–4** is shown to stabilize the charge transfer state compared to the corresponding control compounds revealing its significance in modulating charge transfer properties.

Introduction

Over the years, organic π -conjugated chromophores have been the subject of intense research due to their wide-ranging applications in materials science, optoelectronics, and biomedicine. Among these, the π -conjugated, spatially close, donor-acceptor (D- π -A) push-pull compounds have become one of the successful strategies in the design and synthesis of optoelectronic materials. The strongly interacting D- π -A type push-pull systems can lower the optical band gap and extend the absorption spectrum towards longer wavelengths. Advantageously, the energy levels and band gaps of such push-pull systems can be tuned effectively by the selection of acceptor and donor entities, and π -bridge and spacer.

The triphenylamine (TPA) core is one of the widely used electron-donating units for the construction of C_3 star-shaped molecules due to the sp^3 hybridized orbital of the nitrogen atom. TPA generally shows good electron-donating and high charge-transporting properties. Similarly, another electron donor, phenothiazine (PTZ), is an important class of heterocyclic compound with a slightly non-planar geometry due to the presence of electron-rich nitrogen and sulfur heteroatoms. PTZs have been extensively used for chemical sensors, photovoltaic devices, and organic light-emitting diodes (OLEDs). Phenothiazine as such is a colorless compound with an absorption maxima around 316 nm. The structure of phenothiazine possesses some unique features different from that of a typical triarylamine. The two phenyl groups of phenothiazine are nearly coplanar, allowing the extension of the π -delocalization over the entire molecule. The electron-rich nature of a phenothiazine provides a good relay for the electron migration in multi-modular donor-acceptor systems.

Tetracyanoethylene (TCNE) is a powerful electron acceptor and its reaction with π -conjugated electron-rich alkynes by a [2 + 2] cycloaddition–retroelectrocyclization reaction, according to Diederich's procedure, ³⁴⁻³⁶ results in push-pull systems carrying electron-deficient, tetracyanobutadiene (TCBD) electroactive unit. The strong push-pull effects result in electron polarization (also often termed as ground state charge transfer) resulting in a new low-energy optical transition extending the optical coverage. Making use of the facile reaction and optical properties they have extensively explored building TCBD-substituted push-pull systems, ³⁷⁻⁴⁰ and polymers as promising materials for photovoltaic applications. ⁴¹⁻⁵⁰ Our groups have explored a wide variety of donor-functionalized TCBD-based molecular systems exhibiting novel optical and excited-state properties including ultrafast charge transfer and intervalence charge transfer properties. ⁵¹⁻⁶¹

In the present investigation, making use of the novel electronic and structural properties of TPA, PTZ and TCBD, we have designed, symmetric and asymmetric, multi-modular push-pull systems, **1–4** wherein

the TCBD is positioned between the terminal PTZ and central TPA entities (Figure 1). The number of TCBD entities has been varied to probe their effect on both ground and excited-state properties. Further, the second series of compounds lacking the terminal PTZ, C1–C4, have also been synthesized to investigate the role of terminal PTZ in 1–4 in governing the excited-state charge transfer events. Key findings are summarized in the following paragraphs.

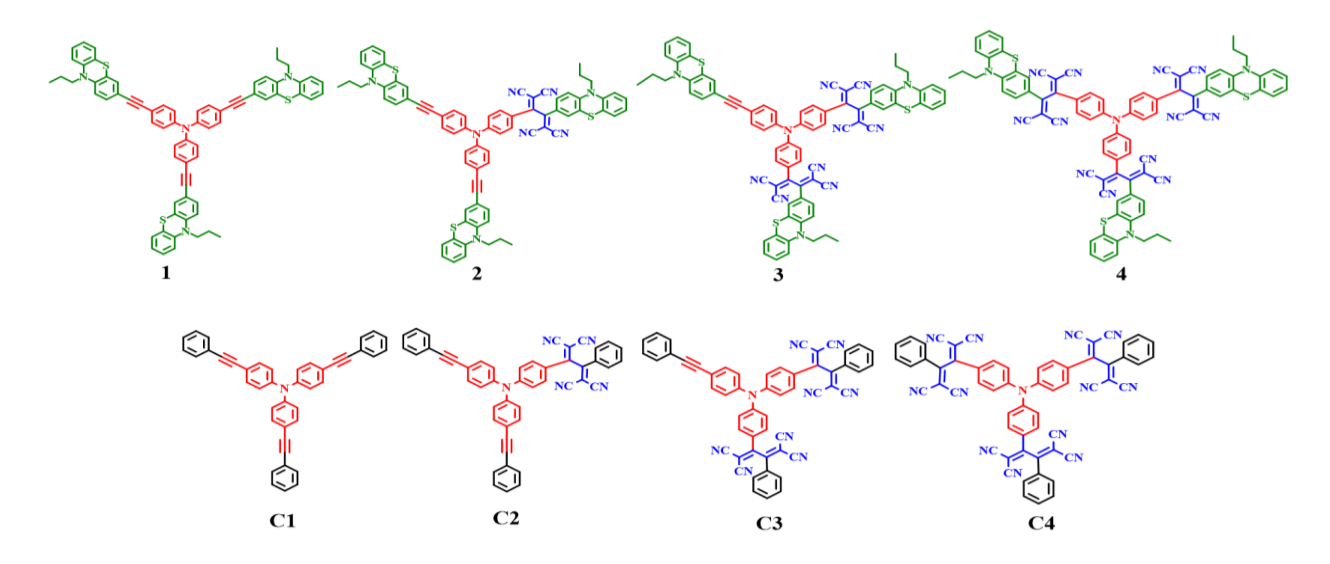


Figure 1. Structure and abbreviation of star-shaped, central triphenylamine derived, phenothiazine-tetracyanobutadiene conjugates, $\mathbf{1}$ – $\mathbf{4}$ (abbreviated as (PTZ-TCBD)₀₋₃-TPA-(PTZ)₀₋₃; (PTZ-TCBD)₀-TPA-(PTZ)₃ = $\mathbf{1}$; (PTZ-TCBD)₁-TPA-(PTZ)₂ = $\mathbf{2}$, (PTZ-TCBD)₂-TPA-(PTZ)₁ = $\mathbf{3}$, and (PTZ-TCBD)₃-TPA-(PTZ)₀ = $\mathbf{4}$] and the control compounds, $\mathbf{C1}$ – $\mathbf{C4}$ (abbreviated as (Ph-TCBD)₀₋₃-TPA; (Ph-TCBD)₀-TPA = $\mathbf{C1}$; (Ph-TCBD)₁-TPA = $\mathbf{C2}$, (Ph-TCBD)₂-TPA = $\mathbf{C3}$ and (Ph-TCBD)₃-TPA = $\mathbf{C4}$) synthesized to probe excited-state charge transfer events.

Experimental Section

General methods

All the chemicals were used as received unless otherwise indicated. All oxygen or moisture-sensitive reactions were performed under a nitrogen/argon atmosphere using the standard Schlenk method. All the chemicals were purchased from commercial sources and used without further purification. 1 H NMR (400 MHz), and 13 C NMR (100 MHz) spectra were recorded on the Bruker Avance (III) 400 MHz, using CDCl₃ as the solvent, and the chemical shifts were reported in parts per million (ppm) with TMS (0 ppm) and CDCl₃ (77.00) as standards. Tetramethylsilane (TMS) was used as reference for recording 1 H (of residual proton; δ = 7.26 ppm), and 13 C (δ = 77.0 ppm) spectra in CDCl₃. UV-visible absorption spectra

of all compounds in Dichloromethane were recorded on a Carry-100 Bio UV-visible Spectrophotometer. Cyclic voltammograms (CVs) were recorded on a CHI620D electrochemical analyzer using Glassy carbon as a working electrode, Pt wire as the counter electrode, and Saturated Calomel Electrode (SCE) as the reference electrode. HRMS was recorded on Brucker-Daltonics, micrO TOF-Q II mass spectrometer.

The UV-visible spectral measurements were carried out with a Shimadzu Model 2550 double monochromator UV-visible spectrophotometer. The fluorescence emission was monitored by using a Horiba Yvon Nanolog coupled with time-correlated single-photon counting with nanoLED excitation sources. A right-angle detection method was used. Differential pulse and cyclic voltammograms were recorded on an EG&G 263A electrochemical analyzer using a three-electrode system. A platinum button electrode was used as the working electrode. A platinum wire served as the counter electrode, and an Ag/AgCl electrode was used as the reference electrode. Ferrocene/ferrocenium redox couple was used as an internal standard. All the solutions were purged prior to electrochemical and spectral measurements using argon gas.

Femtosecond transient absorption spectroscopy experiments were performed using an ultrafast femtosecond laser source (Libra) by Coherent incorporating a diode-pumped, mode locked Ti: sapphire laser (Vitesse) and a diode-pumped intracavity doubled Nd:YLF laser (Evolution) to generate a compressed laser output of 1.45 W. For optical detection, a Helios transient absorption spectrometer coupled with a femtosecond harmonics generator, both provided by Ultrafast Systems LLC, was used. The sources for the pump and probe pulses were derived from the fundamental output of Libra (Compressed output 1.45 W, pulse width 100 fs) at a repetition rate of 1 kHz; 95% of the fundamental output of the laser was introduced into a TOPAS-Prime-OPA system with a 290–2600 nm tuning range from Altos Photonics Inc., (Bozeman, MT), while the rest of the output was used for generation of a white light continuum. Kinetic traces at appropriate wavelengths were assembled from the time-resolved spectral data. Data analysis was performed using Surface Xplorer software supplied by Ultrafast Systems. All measurements were conducted in degassed solutions at 298 K. The estimated error in the reported rate constants is ±10%.

Synthesis

TPA-PTZ 1: Under argon atmosphere a solution of tris-(4-iodophenyl)amine (1a) (0.5 g, 0.80 mmol) and the corresponding 3-ethynyl-10-propyl-10*H*-phenothiazine (1b) (0.85 g, 3.2 mmol) in dry THF (50 ml), added triethylamine (15 ml), Pd(PPh₃)₄ (0.046 g, 0.04 mmol), CuI (0.007 g, 0.04 mmol), stirred for 16 h at 65 °C. After completion of the reaction, the reaction mixture was concentrated under reduced pressure,

the crude compound was purified by column chromatography on silica, using Hexane/ DCM (80:20), and afforded pure compound **TPA-PTZ 1** around 66 % yield. Yellow solid (0. 550 g, 66 %). ¹**H NMR (CDCl₃, 400 MHz, ppm)**: δ 7.39 (d, J = 8 Hz, 6H), 7.29-7.27 (m, 5H), 7.16-7.11 (m, 6H), 7.05 (d, J = 8 Hz, 7H), 6.92 (t, J = 8 Hz, 3H), 6.85 (d, J = 8 Hz, 3H), 6.78 (d, J = 8 Hz, 3H), 3.81 (t, J = 8 Hz, 6H), 1.87-1.79 (m, 6H), 1.01 (t, J = 8 Hz, 9H). ¹³**C NMR (CDCl₃, 100 MHz, ppm)**: 146.4, 145.1, 144.7, 144.6, 143.8, 132.6, 130.8, 130.1, 130.0, 129.9, 129.6, 127.4, 127.2, 126.5, 124.7, 124.2, 124.0, 123.9, 122.6, 118.0, 117.1, 116.6, 115.4, 115.1, 115.0, 114.7, 89.0, 88.7, 49.2, 20.0, 11.2. **HRMS (ESI-TOF)**: m/z calculated for C₆₉H₅₄N₄S₃ 1034.3505 [M]⁺, measured 1034.3504 [M]⁺.

TPA-PTZ 2: In a 50 mL round-bottomed flask, tetracyanoethylene (TCNE, 12 mg, 0.09 mmol) was added to solution of **TPA-PTZ 1** (100 mg, 0.09 mmol) in DCM (20 mL). The reaction mixture was stirred at room temperature for 4 h. After completion of the reaction, the reaction mix. was dried under vacuum and purified by column chromatography with hexane/DCM (40:60, v/v) as eluent to give compound **TPA-PTZ 2** as dark red solid (yield: 70 mg, 62%). ¹**H NMR (400 MHz, CDCl₃):** δ 7.73 (d, J = 8 Hz, 1H), 7.65 (d, J = 8 Hz, 2H), 7.49 (d, J = 8 Hz, 4H), 7.42-7.29 (m, 6H), 7.22-6.84 (m, 16 H), 6.79 (d, J = 8 Hz, 2H), 6.73-6.88 (m, 2H), 3.87-3.76 (m, 6H), 1.88-1.76 (m, 6H), 1.06-0.98 (m, 9H). ¹³C **NMR (CDCl₃, 100 MHz, ppm)**: δ 153.1, 152.6, 151.1, 150.6, 145.4, 145.1, 144.5, 144.3, 144.1,144.0, 143.9, 143.7, 142.0, 141.3, 133.0, 132.9, 131.7, 130.9, 130.7, 130.4, 130.3, 130.2, 130.1, 130.0, 129.6, 127.9, 127.8, 127.6, 127.4, 127.3, 127.0, 126.8, 126.4, 126.2, 126.1, 125.3, 125.1, 124.9, 124.8, 124.7, 124.4, 124.1, 124.1, 122.7, 121.4, 119.7, 118.9, 117.2, 116.9, 116.8, 116.6, 116.1, 115.5, 115.2, 115.2, 115.0, 114.8, 113.4, 113.2, 112.8, 112.2, 112.0, 89.8, 88.5, 81.5, 80.7, 49.3, 49.2, 20.0 19.9, 11.2, 11.2; **HRMS (ESI, positive)** m/z [M] + calculated for $C_{75}H_{54}N_8S_3$ 1162.3628, found 1162.3844 [M]+.

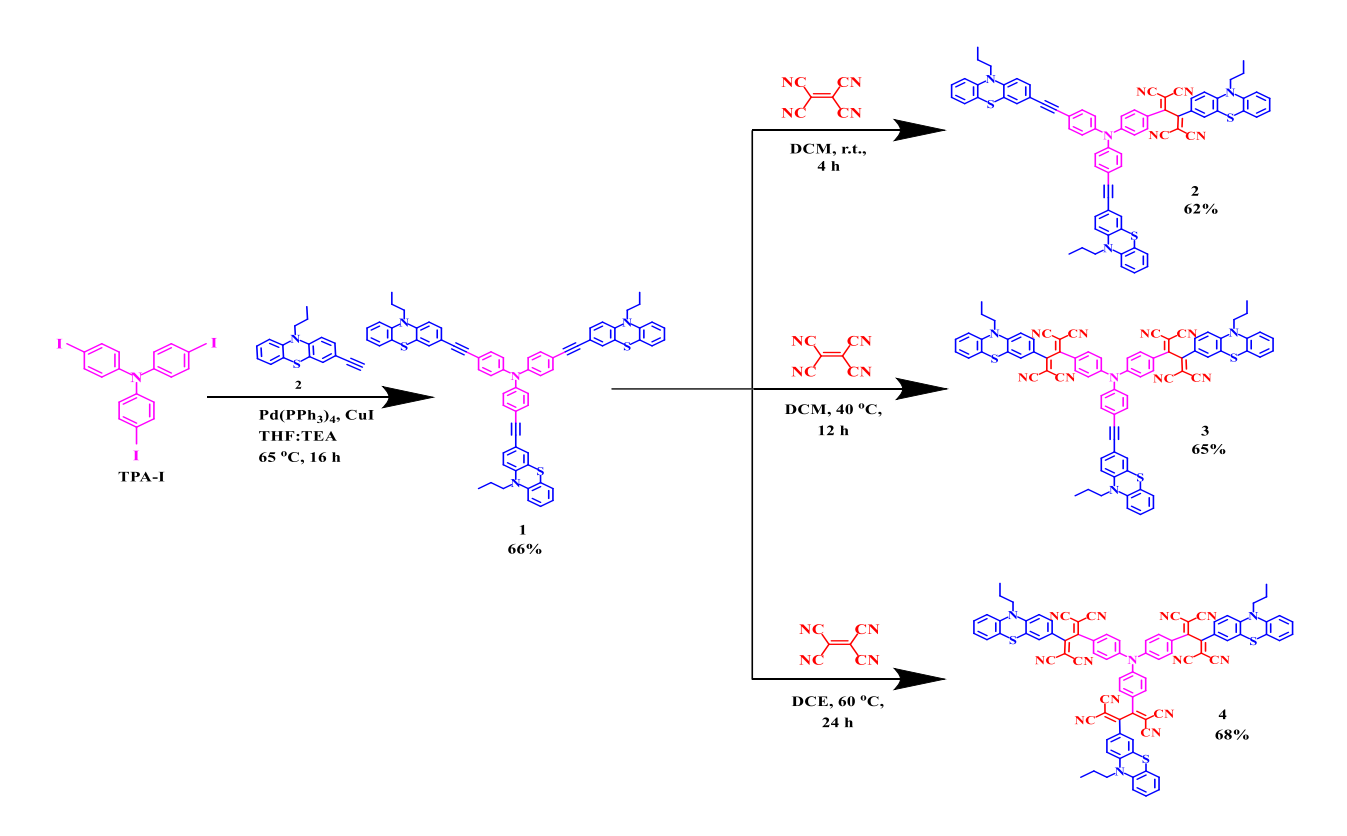
TPA-PTZ 3: In a 50 mL round-bottomed flask, tetracyanoethylene (TCNE, 24 mg, 0.19 mmol) was added to a solution of **TPA-PTZ 1** (100 mg, 0.09 mmol) in DCE (20 mL). The reaction mixture was heated at 40 °C for 12 h. After completion of the reaction, the reaction mix. was dried under vacuum and purified by column chromatography with hexane/DCM (20:80, v/v) as eluent to give **TPA-PTZ 3** as a dark red solid (yield: 80 mg, 65%). ¹**H NMR (400 MHz, CDCl₃):** δ 7.73-7.67 (m, 7H), 7.55 (d, J = 8 Hz, 1H), 7.47 (t, J = 8 Hz, 1H), 7.38-7.29 (m, 4H), 7.22-7.15 (m, 10H), 7.08-6.99 (m, 4H), 6.90-6.87 (m, 4H), 6.79 (d, J = 8 Hz, 1H), 6.74-6.68 (m, 1H), 3.88-3.76 (m, 6H), 1.88-1.78 (m, 6H), 1.06-0.99 (m, 9H). ¹³**C NMR (CDCl₃, 100 MHz, ppm):** δ 165.1, 163.7, 151.3, 150.8, 143.6, 141.8, 141.1, 133.5, 131.5, 131.0, 130.7, 130.5, 130.4, 130.2, 130.0, 129.9, 129.6, 127.7, 127.6, 127.4, 127.1, 125.5, 124.8, 124.7, 124.5, 124.3, 123.2, 123.1, 122.8, 122.4, 117.3, 116.9, 116.7, 116.2, 115.3, 115.2, 115.1, 114.9, 112.8, 112.5, 112.4, 112.1, 111.7, 83.2, 80.4, 49.9, 49.3,

20.0, 19.9, 11.1, 11.1; **HRMS (ESI-TOF):** m/z calculated for $C_{81}H_{54}N_{12}S_3$ 1290.3751 [M]⁺, measured 1290.3761 [M]⁺.

TPA-PTZ 4: In a 50 mL round-bottomed flask, tetracyanoethylene (TCNE, 49 mg, 0.09 mmol) was added to a solution of **TPA-PTZ 1** (100 mg, 0.38 mmol) in DCE (20 mL). The reaction mixture was heated at 60 °C for 24 h. After completion of the reaction, the reaction mix. was dried under vacuum and purified by column chromatography with hexane/DCM (10:90, v/v) as eluent to give **TPA-PTZ 4** as a dark red solid (yield: 93 mg, 68%). ¹**H NMR (400 MHz, CDCl₃):** δ 7.73-7.71 (m, 9H), 7.37 (t, J = 4 Hz, 3H), 7.29-7.27 (m, 5H), 7.25 (s, 4H), 7.20-7.17 (m, 3H), 7.08-6.99 (m, 3H), 6.92-6.88 (m, 5H), 6.73 (d, J = 8 Hz, 1H), 3.89-3.81 (m, 6H), 1.91-1.79 (m, 4H), 1.06-1.02 (m, 9H). ¹³**C NMR (CDCl₃, 100 MHz, ppm):** δ 165.3, 165.1, 163.2, 163.0, 151.5, 151.0, 149.7, 149.7, 149.7, 141.6, 141.0, 131.7, 130.7, 130.5, 130.4, 129.9, 128.0, 127.8, 127.7, 127.6, 127.6, 127.5, 125.6, 125.2, 125.1, 124.7, 124.4, 124.6, 122.4, 117.4, 117.0, 116.3, 115.4, 115.1, 112.7, 112.5, 112.2, 112.0, 116.3, 115.4, 115.1, 112.7, 112.5, 112.2, 112.0, 111.2, 81.1, 80.3, 80.3, 50.1, 20.0, 11.1; **MALDI** calculated for $C_{87}H_{54}N_{16}S_3$ 1418.3879 [M]⁺, measured 1419.455.

Results and Discussion

Scheme 1 shows the developed synthetic scheme for compounds 1–4 while details are presented in the experimental section. Briefly, the symmetrical compound 1 was synthesized by the Pd-catalyzed Sonogashira cross-coupling of tris-(4-iodophenyl)-amine (1a) and corresponding 3-ethynyl-10-propyl-10*H*-phenothiazine (1b) in the presence of Pd(PPh₃)₄ and CuI in degassed THF: TEA (1:1) under argon atmosphere at 65 °C for 16 h which resulted in 1 at 66% yield. The TCBD functionalized symmetrical and unsymmetrical compounds 2–4 were synthesized via [2+2] cycloaddition-retro-electrocyclization reaction with the strong electron acceptor TCNE.²⁸ The reaction of symmetrical 1 with one equivalent of TCNE in DCM at room temperature for 4 h resulted in an exclusive mono- TCBD substituted unsymmetrical compound 2 in 62% yield. Similarly, the reaction of symmetrical 1 with two equivalents of TCNE in DCM solvent at 40 °C for 12 h resulted in di-TCBD substituted unsymmetrical 3 in 65% yield, whereas increasing the reaction temperature to 60 °C for 24 h using four equivalents of TCNE with symmetrical 1 in DCE solvent resulted in tri-TCBD substituted symmetrical 4 in 68% yield.



Scheme 1. Synthetic scheme of compounds 1-4.

The control compounds, **C1–C4** were synthesized according to the earlier reported procedure. ⁶² All of the reported compounds were purified through silica gel (100-200 mesh) column chromatography using Hexane: DCM solvent and thoroughly characterized by ¹H, ¹³C NMR, and high-resolution mass spectroscopy (HRMS) techniques. (see SI for spectral details, Figures S1 – S12).

Absorption and emission properties of compounds **C1–C4** and **1–4** were subsequently investigated to evaluate the effect of TCBD in these compounds and the role of the second electron donor, PTZ in **1–4**. Compound **C1** revealed a single absorption band located at 372 nm (see Table 1 for spectral data). The introduction of TCBD resulted in two peaks, the first one in the 300–340 nm range and the second one in the 450-650 nm range (see Figure 2a). The first one was attributed to the normal π – π * transition while the second one was for the ground state charge transfer (or charge polarization, TCBD $^{\delta}$ –TPA $^{\delta+}$). Importantly, as the number of TCBD entities increased, a systematic blue-shift of both peak maxima was witnessed. Interestingly, the introduction of the second electron donor, PTZ revealed better optical coverage in **2–4** extending the absorption well into the near-IR region (Figure 2b). The spectrum of **1** revealed two peaks, the first one as a shoulder-type peak at 330 nm while the second one at 394 nm. Introducing the TBCD revealed a total of three absorption bands, two in the 300–420 nm region

attributable to the π - π^* transitions of the PTZ and TPA entities and a broader peak in the 420–750 nm range due to charge polarization. Similar to **C2–C4**, with the increase in TCBD entities in **2–4**, a systematic blue shift was observed for both types of peaks suggesting that the PTZ is involved in the charge polarization, that is, the formation of $PTZ^{\delta-}$ - $TCBD^{\delta-}$ -TPA type species (with some contributions from TPA, *vide supra*).

Table 1. Absorption and luminescence spectral details of the investigated compounds in DCB.										
Compound	Absorption, nm	Fluorescence, nm	Phosphorescence,							
C1	373	417	698							
C2	343 431 512									
С3	314 395 520									
C4	303 497 517									
1	323 393	<mark>470</mark>	<mark>701</mark>							
2	322 365 520									
3	318 390 525									
4	315 385 504									

Among the investigated compounds only **C1** and **1** were found to be luminescent upon excitation of the samples corresponding to the π - π * peak maxima (Figure 2c). Fluorescence maxima of **C1** were located at 416 nm while that of **1** was located at 470 nm. Direct excitation of the charge transfer peaks in the visible region and extending the monitoring window did not show new peaks corresponding to charge transfer emission. It is likely that the intensities of such peaks are low. Lifetimes of **C1** and **1** determined from the time-correlated single counting technique were found to be 2.89 ns for **C1** and 2.59 ns for **1** (see Figure S13 for delay plot). Phosphorescence of both **C1** and **1** was also recorded at liquid nitrogen temperature (Figure 2d). Peak maxima of **C1** were located at 698 nm while that of **1** was at 701 nm.

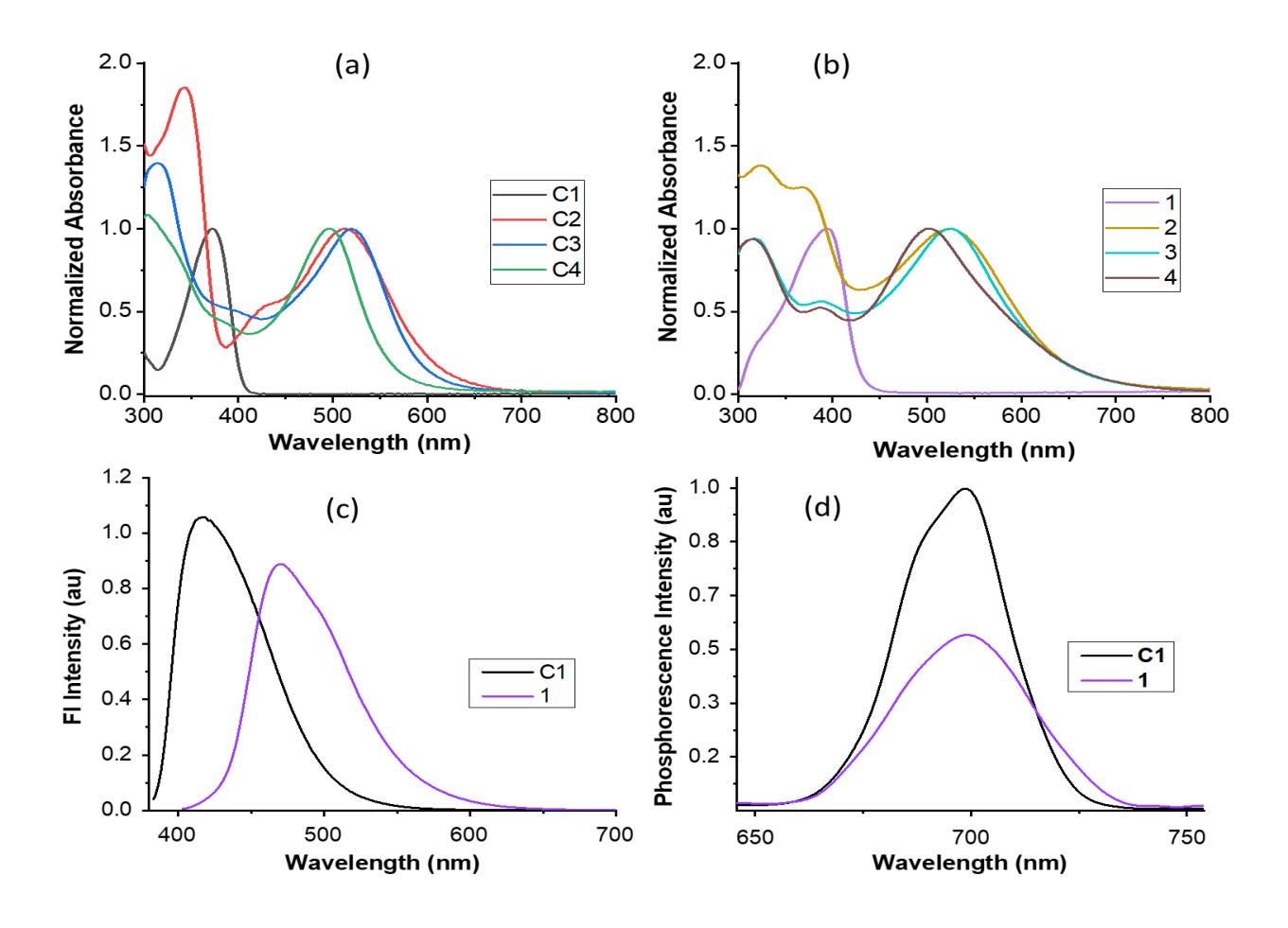


Figure 2. Absorption (a and b), fluorescence (c), and phosphorescence (d) spectra of the indicated compounds in DCB. Phosphorescence was recorded at 77K. The samples were excited at peak maxima located in the 300-400 nm region of the corresponding compound (see Table 1).

Next, electrochemical studies using both cyclic (CV, to check reversibility) and differential pulse voltammetry (DPV, for peak potential measurement) were performed in DCB containing 0.1 M (TBA)ClO₄. CVs and DPVs are shown in Figures S14 and S15, respectively, while the data are summarized in Table 2. The first oxidation of C1 bearing only TPA was located at 1.12 V vs. Ag/AgCl while for 1 having both PTZ and TPA, oxidation at 0.94 and 1.19 V was observed, and by comparison, the first oxidation to the PTZ entity and the second one to TPA entity was possible to arrive. The electron-deficient TCBD is known to reveal two one-electron reductions, this seems to be the case in the C2–C4 and 2–4 series. In the case of C2–C4, the first reduction of TCBD was located at -0.19, -0.14, and -0.11 V, that is, TCBD reduction progressively became easier. Importantly, in the case of C3 and C4, the first reduction was a split peak, suggesting electron exchange between the TCBD entities. ⁵⁶ On the oxidation side, the first oxidation of

C2–C4 was located at 1.35, 1.46, and 1.67 V. This was also the trend for subsequent oxidations. That is, increasing the TCBD entities, made the oxidation process gradually harder. The electrochemical redox gap ($\Delta E_{1/2}$), that is, the potential difference between the first oxidation and first reduction was 1.54 V for C2, 1.60 V for C3, and 1.78 V for C4. This trend was consistent with the blue shift observed along with the series in the optical absorption spectral studies. Such a trend was also observed for compounds 2–4, however, due to facile reduction of PTZ over TPA, the measured $\Delta E_{1/2}$ were even smaller. $\Delta E_{1/2}$ values of 1.15 V for 2, 1.19 V for 3, and 1.22 V for 4 were observed, a trend that was also consistent with red-shift optical coverage of 2–4 compared to C2–C4, and comparatively shrinking of the gap along with series due to increased number of TCBD entities. ⁵⁶ It is of significance to note reduced $\Delta E_{1/2}$ with the addition of the second electron donor in the investigated series of compounds, 2–4.

Table 2. Electrochemical redox potentials of the investigated compounds in DCB containing 0.1 M (TBA)ClO ₄ .										
	$\Delta E_{1/2}$, V									
compound			E_{ox}			E_{red}				
C1	1.12	1.62						> 3.0		
1	0.94	1.19	1.51					> 3.0		
C2	1.35	1.67			-0.19	-0.59		1.54		
2	0.87	1.03	1.27	1.44	-0.28	-0.60		1.15		
С3	1.46	1.44	1.56		-0.14	-0.26	-0.65	1.60		
3	1.03	1.38	1.64	1.83	-0.16	-0.29	-0.67	1.19		
C4	1.67				-0.11	-0.24	-0.60	1.78		
4	1.03	1.38	1.63	1.89	-0.19	-0.31	-0.62	1.22		

Geometry optimization followed by generating frontier orbitals to visualize donor-acceptor push-pull sites within the studied molecules was performed. For this, the structures were optimized on the B3LYP/6-31G* basis set, and functional,⁶³ and frontier HOMO and LUMO were generated, as shown in Figure 3. As expected, the HOMO of both **C1** and **1** were spread all over the molecules. In the case of **C2** and **2**, HOMO spreading on the TPA and PTZ-TPA arms away from the TCBD entity and LUMO on TCBD was obvious. This

trend was also observed for C3 and 3, where HOMO on TPA and PTZ-TPA arms lacking TCBD was witnessed (more on the PTZ site). The LUMOs were on both TCBD entities. In the case of C4 and 4, HOMO on the central TPA and PTZ-TCBD arm, and LUMO on two of the TCBD entities were witnessed. These results reveal charge transfer type interactions in C2–C4 and 2–4 involving neighboring TPA/PTZ electron donor and TCBD electron acceptor. Importantly, in cases 2 and 3, the presence of HOMO on free PTZ and LUMO on TCBD with a center-to-center distance of 16.4 Å was possible to arrive. In this instance, selective excitation of the free-PTZ entity could result in charge separation.

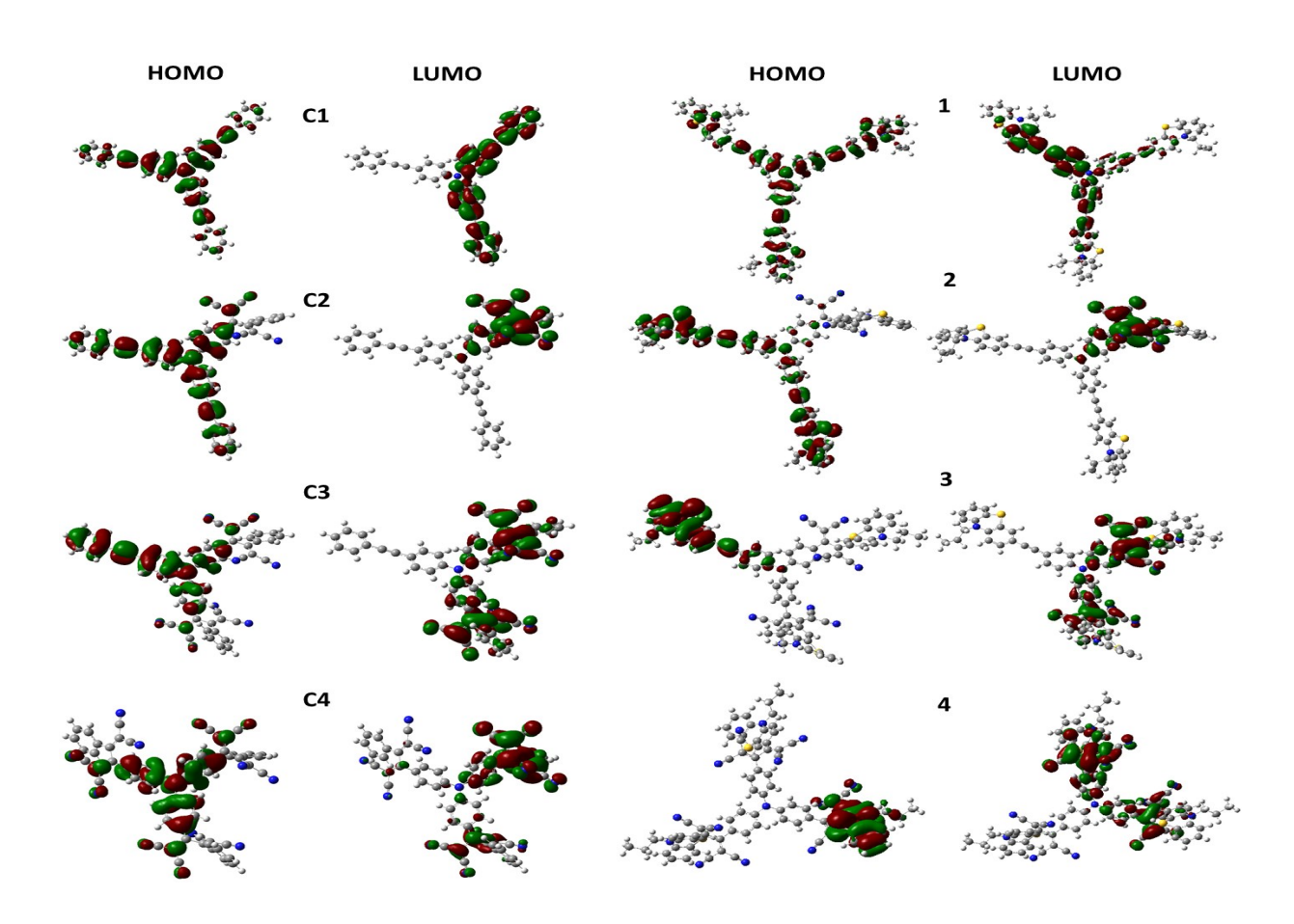


Figure 3. Frontier HOMO and LUMO on B3LYP/6-31G* optimized structure of the investigated compounds.

From the spectral, luminescence, computational, and electrochemistry data, energy level diagrams were established to visualize different photochemical events in the studied push-pull systems (Figure 4). The HOMO–LUMO energy gap from the computational studies was used as the energy of the CT state, E_{CT}

in the energy diagram. The energy of the charge-separated state in benzonitrile was calculated according to the Rehm-Weller approach ⁶⁴ using optical and electrochemical data according to equations i-iii

$$-\Delta G_{\rm CR} = E_{\rm ox} - E_{\rm red} + \Delta G_{\rm S} \tag{i}$$

$$-\Delta G_{\rm CS} = \Delta E_{00} - (-\Delta G_{\rm CR})$$
 (ii)

where ΔE_{00} corresponds to the singlet state energy of 1. The term ΔG_{S} refers to electrostatic energy calculated according to the dielectric continuum model (see equation iii). The E_{ox} and E_{red} represent the oxidation potential and the first reduction potential, respectively.

$$\Delta G_{\rm S} = {\rm e}^2/4 \, \pi \varepsilon_{\rm o} \, [-1/{\rm R}_{\rm cc} \, \varepsilon_{\rm R})$$
 (iii)

The symbols ε_0 and ε_R represent the vacuum permittivity and dielectric constant of DCB used for photochemical and electrochemical studies (= 9.93). R_{CC} is the center-to-center distance between donor and acceptor entities from the computed structures. The energy of charge transfer was calculated from the peak maxima of the charge transfer peak.

In the case of compounds **C2–C4** (see Figure 4a), excitation of TPA corresponding to its $\pi - \pi$ (locally excited, LE) peak maxima, would populate the singlet excited state ¹[(Ph-TCBD)₁₋₃-TPA]* having enough energy to promote the charge transfer event to yield $(Ph-TCBD)_{1-3}^{\delta-}-TPA^{\delta+})$. Direct excitation of the CT band would produce the singlet excited state of the charge transfer state, ${}^{1}[(Ph-TCBD)_{1-3}{}^{\delta-}-TPA^{\delta+})]^{*}$. In a polar solvent such as benzonitrile, the CT state could undergo the charge-separated (CS) state producing radical ion-pairs, (Ph-TCBD)₁₋₃⁻-TPA⁻⁺) in competition with populating the low-lying triplet excited state, ³[(Ph-TCBD)₁₋₃-TPA]*. A relatively complex situation arises in compounds **2–4** due to the presence of PTZ with and without connected TCBD entity(ies) (Figure 4b). In this instance, the ¹[(PTZ-TCBD)₁₋₃-TPA- $(PTZ)_{0.2}$]* state produced by LE excitation would promote the CT state to produce $(PTZ-TCBD)_{1.3}\delta^--TPA$ - $(PTZ)_{0-2}^{\delta+}$. Direct excitation corresponding to CT peak maxima, could also populate the ${}^{1}[(PTZ-TCBD)_{1-3}]$ $TPA-(PTZ)_{0-2}$ state. From the location of the frontier orbitals, formation of ${}^{1}[(PTZ-TCBD)^{\delta-}-TPA (PTZ)_2^{\delta+}$ in the case of **2**, formation of ${}^1[(PTZ-TCBD)_2^{\delta-}-TPA-(PTZ)^{\delta+}]^*$ in the case of **3**, and formation of ${}^{1}[(PTZ-TCBD)_{3}^{\delta-}-TPA^{\delta+}]^{*}$ in the case of 4 could be envisioned. Since the energy of these CT states is higher than CS state, the resulting CT state could populate the triplet state or end up producing charge separates states, viz., [(PTZ-TCBD)⁻-TPA-(PTZ)₂⁺ in the case of **2**, (PTZ-TCBD)₂⁻-TPA-(PTZ)⁺ in the case of **3**, and $(PTZ-TCBD)_3$ --TPA in the case of **4**. A charge-separated state may be preferred in cases 2 and 3 due to the distal positioning of the free PTZ and PTZ-TCBD, donor, and acceptor entities.

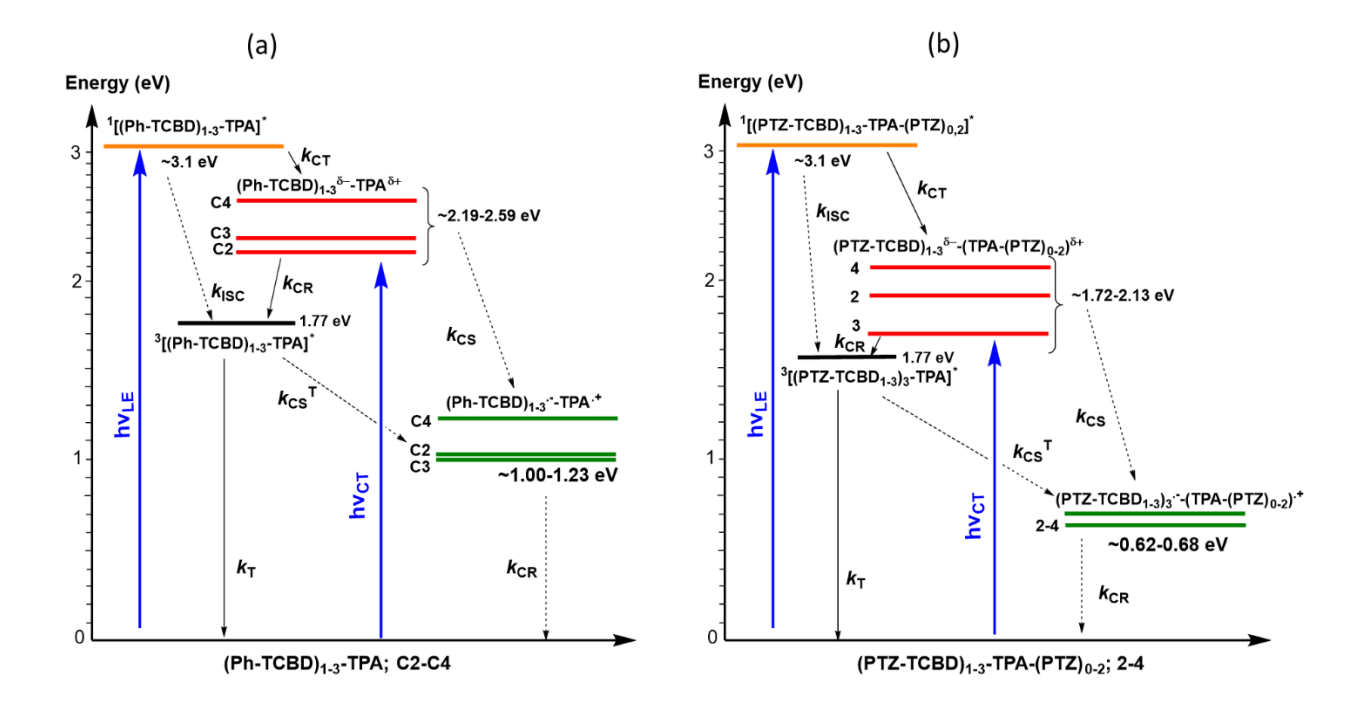


Figure 4. Energy level diagram demonstrating excited charge transfer and charge separation events upon photoexcitation of **C2–C4** and **2–4** push-pull systems. The energy of the charge transfer states, (Ph-TCBD)₁₋₃ $^{\delta-}$ -TPA $^{\delta+}$ in the case of **C2–C4**, and (PTZ-TCBD)₁₋₃ $^{\delta-}$ -TPA-(PTZ)₀₋₂ $^{\delta+}$ in the case of **2–4** are the energy difference between the respective HOMO and LUMO levels arrived from the DFT calculations. Under the conditions of λ_{CT} excitation, the excited state species is the excited singlet charge transfer complex, 1 [(Ph-TCBD)₁₋₃ $^{\delta-}$ -TPA $^{\delta+}$)]* in the case of **C2–C4** and 1 [(PTZ-TCBD)₁₋₃ $^{\delta-}$ -TPA-(PTZ)₀₋₂ $^{\delta+}$]* in the case of **2–4**; not shown in the diagram for brevity. The energy of the charge-separated states was calculated according to the Rehm-Weller approach in DCB.

In an effort to arrive at the spectrum of the charge transfer/separation species, spectroelectrochemical studies on both series of compounds, viz., C2–C4, and 2–4 were performed. For this, spectral data during the process of first oxidation and first reduction for each compound was recorded by applying appropriate potentials (100 mV past the redox peak potentials). The final spectrum of the cation and anion were digitally added and subtracted with the neutral species to generate the differential absorption spectrum corresponding to the charge transfer/separation species. Figure S16 in SI shows the spectrum for each push-pull system generated in this fashion. The main features involved depleted peaks in the 300-340 nm range and 500-515 nm range. For compounds 2–4, another depleted peak in the 380–390 nm range was also observed. Should there is excited-state charge transfer/separation in these push-pull systems, the spectrum of the transient species corresponding to

the CT state should match closely with that of the spectrum arrived from spectroelectrochemical studies.

Having detailed the possible photochemical events in the studied push–pull systems as summarized above, next, transient pump-probe spectral studies were performed using both LE and CT excitation wavelengths. Figures S17a and b in SI show the femtosecond transient absorption (fs-TA) spectra of C1 and 1 (having no TCBD) in benzonitrile, respectively, along with the decay-associated spectra (DAS) and species associated spectra (SAS) from Glotaran analysis⁶⁵⁻⁶⁶ of the transient data. In the case of C1, the singlet excited state (S₁) species obtained within the first 6–7 ps revealed a broad excited state absorption (ESA) peak at 527 nm. The decay of this peak was associated with another less intense broad peak with maxima at 540 nm. A two-component fit was representing the initial S₁ and a triplet excited state, T₁ formed from the process of intersystem crossing (ISC) was satisfactory whose DAS and SAS spectra are shown on the right-hand side of Figure S17a. The lifetime of the T₁ state was 1.76 ns suggesting the formation of a short-lived triplet excited state. In the case of 1, the S₁ state formed within the first 2–3 ps, revealed ESA peaks at 623 nm. With time, a blue shift accompanied decay and a new peak at 412 nm was witnessed. A two-component fit was representing the initial S₁ and the T₁ state was satisfactory whose DAS and SAS spectra are shown on the right-hand side of Figure S17b. The lifetime of the T₁ state was found to be 2.20 ns, not significantly different from that of C1.

Next, photophysical properties of the relatively simpler version of push-pull systems, C2-C4 were performed in polar benzonitrile as the charge separation process is favored in polar solvents (Figure 5). The samples were excited at 350 nm corresponding to the LE excitation. In all three systems, the S₁ species formed within the first 1-3 ps, revealed two main ESA peaks, the first one in the 490 nm region and the second one in the 630 nm range. There was a systematic blue shift of the first peak with the increase in the TCBD entities, that is, peak locations at 498 nm for C1, 481 nm for C2, and 478 nm for C3 were witnessed. The decay of this peak was associated with an initial negative signal in the 500 nm range, and the recovery of this signal was associated with a new peak in the 550 nm range. The DAS and SAS spectra for each compound are shown on the right-hand side. A three-component fit representing $S_1 \rightarrow CT \rightarrow T_1$ was satisfactory. The DAS spectra in the middle panel nicely demonstrate the sequential occurrence of these events while the SAS spectrum attributed to the CT state (red trace) agreed well with the spectrum deduced for the CT state from spectroelectrochemical studies (dashed magenta line). These results unequivocally prove the occurrence of CT in C2-C4 in DCB. In all these systems, the spectrum attributed to the T_1 state (blue line) was almost similar and agreed with that observed for C1 in Figure S17a. The time constants of the CT states (average lifetime of the state) were 8.43, 22.09, and 24.14 ps, respectively for C2, C3, and C4, that is, with an increase in the number of TCBD entities, improved lifetimes for the CT states to some extent were witnessed. Lifetimes of the T_1 state were in the range of 1-3 ns. Compounds C2–C4 were also excited at 500 nm corresponding to the charge transfer band (see Figure S18). The instantaneously formed ${}^1[(Ph\text{-}TCBD)_{1\cdot3}{}^{\delta-}\text{-}TPA^{\delta+})]^*$ was characterized by an ESA peak in the 602-606 nm range, and a negative peak in the 510-520 nm range, expected for the CT state from the earlier discussed spectroelectrochemical data. A two-component fit was satisfactory in the Glotaran analysis whose DAS and SAS are shown in Figure S18 on the right-hand side of the corresponding transient spectra. The first state, the singlet excited CT state revealed lifetimes of 5.82, 11.82, and 34.47 ps, respectively, for C2, C3, and C4, lightly lower than those observed for the CT state time constants for the samples excited at 350 nm corresponding to LE state. The spectral features of the second component were that of the T1 state, however, the time constants were much smaller in the range of 55-81 ps. The data were also subjected to a three-component fit to seek any long-lived component representing the charge-separated state. However, no strong evidence of charge-separated product could be obtained.

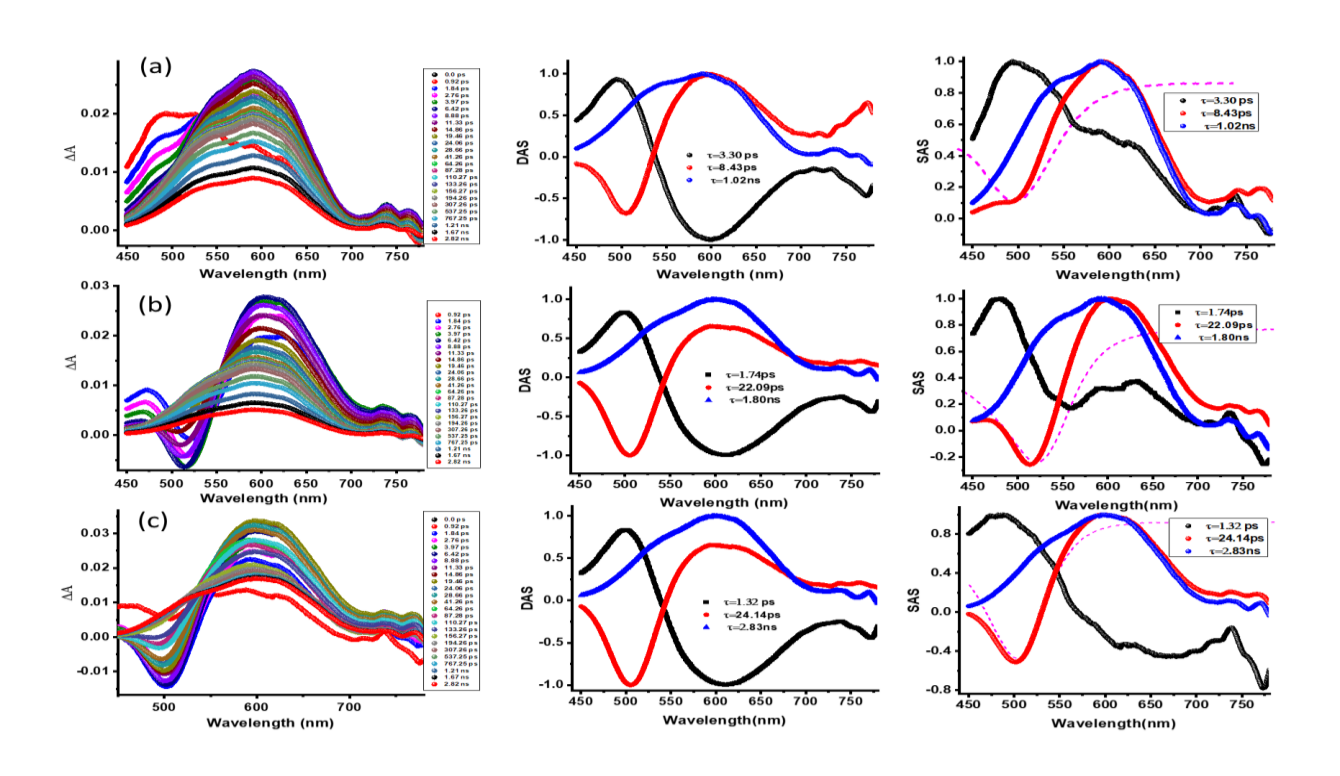


Figure 5. Fs-TA spectra at the indicated delay times of compounds C2–C4 in benzonitrile (λ_{ex} = 350 nm). Decay and species-associated spectra from Glotaran analysis are shown on the right-hand side. The dashed line in the SAS panel corresponds to the spectrum deduced for the CT state from spectroelectrochemical studies.

Next, transient spectra of compounds **2–4** were recorded in benzonitrile, excited at 393 nm corresponding to the LE state. Figure 6 shows the spectral data along with the DAS and SAS from Glotaran analysis. The ${}^1[(PTZ-TCBD)_{1-3}-TPA-(PTZ)_{0-2}]^*$ formed within the first few ps was characterized by an ESA peak at 620-640 nm range along with a negative peak in the 500 nm range. The decay of the ESA peak was accompanied by a blue shift along with a shoulder peak in the 540 nm range. A three-component fit in Glotaran representing $S_1 \rightarrow CT \rightarrow T_1$ was satisfactory whose spectra are shown on the respective right-hand side. As observed for compounds **C2–C4**, the SAS spectrum obtained for the T_1 state was in agreement with what was observed for compound **1**. Importantly, the SAS spectrum corresponding to the CT state matched well with that arrived from spectroelectrochemical results. Time constants of the CT state were 24.94, 43.10, and 57.89 ps, respectively, for **1**, **2**, and **3**. Importantly, these values were much higher than that observed for **C2–C4** lacking the terminal electron donor, PTZ. The T_1 state had time constant values ranging between 880-910 ps. The data was also subjected to four-component fits, both sequential and simultaneous modes to seek any long-lived CS states. However, no such events could be observed suggesting that the CT state transforms into the corresponding triplet state, as shown in the energy diagram in Figure 4.

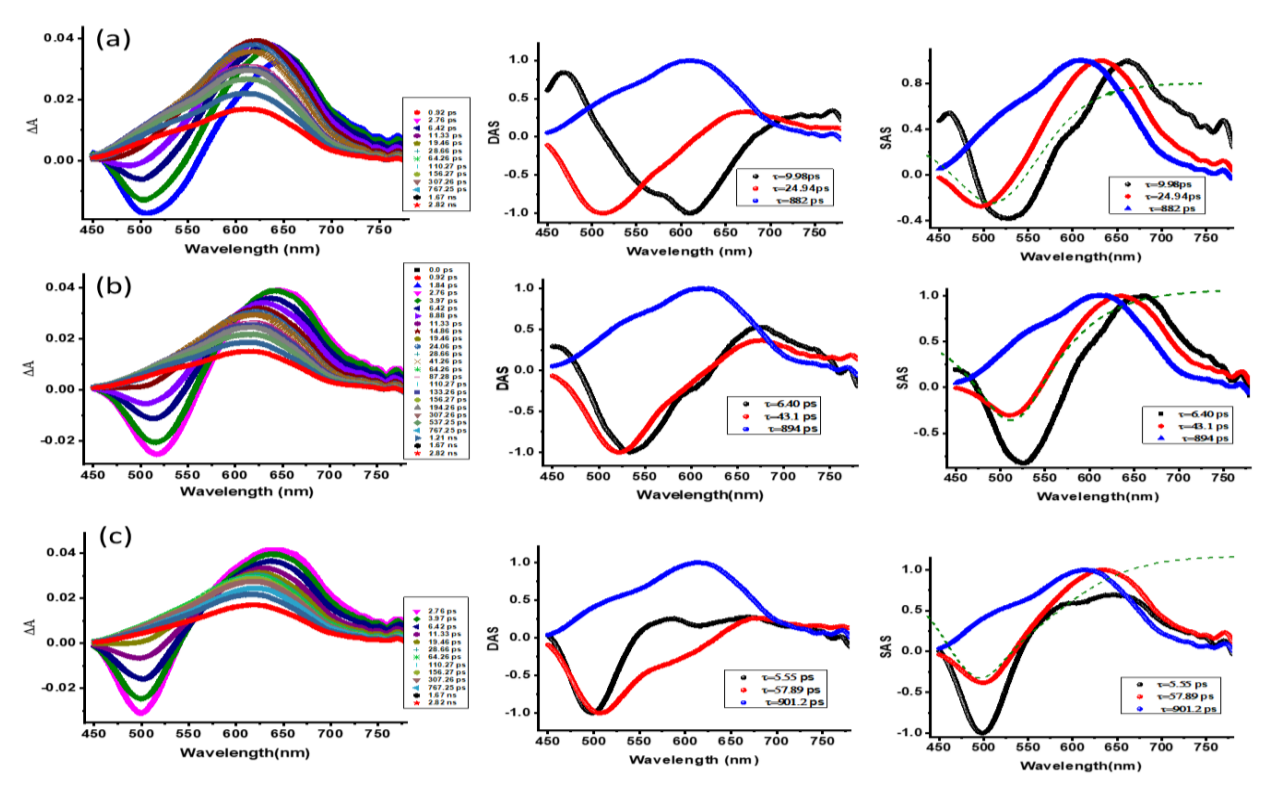


Figure 6. Fs-TA spectra at the indicated delay times of compounds **2–4** in benzonitrile (λ ex = 393 nm). Decay and species-associated spectra from Glotaran analysis are shown on the right-hand side. The

dashed line in the SAS panel corresponds to the spectrum deduced for the CT state from spectroelectrochemical studies.

Finally, compounds **2–4** were also excited at 500 nm corresponding to the CT state, as shown in Figure S19. The 1 [(PTZ-TCBD) ${}_{1\cdot3}{}^{\delta-}$ -TPA-(PTZ) ${}_{0\cdot2}{}^{\delta+}$]* formed revealed an ESA peak in the 650 nm region and a negative peak in the 500 nm range. Decay/recovery of these peaks was associated with a new peak in the 600 nm region suggesting that the 1 CT* transforms into a T_{1} state prior to returning to the ground state. A two-component analysis representing 1 CT* \rightarrow T_{1} was satisfactory in these systems, as shown by DAS and SAS spectra on the right-hand panels. Time constants for the 1 CT* states were found to be 5.74, 7.09, and 8.32 ps, much small than when the samples were excited at their respective LE states. Importantly, with an increase of TCBD entities, time constants for CT state improved. The time constants for the T_{1} state also followed such a trend with the highest time constants of about 600 ps in the case of **4**.

Conclusions

In summary, a novel series of push-pull systems by introducing a powerful electron acceptor, TCBD between the donor entities of a C3 symmetric TPA-(PTZ)₃ molecular scaffold has been synthesized via Pdcatalyzed Sonogashira cross-coupling reaction, followed by [2+2] cycloaddition-retroelectrocyclization reaction. As a control, a TPA scaffold lacking PTZ was also synthesized. The number of TCBD entities was varied between 1 and 3 in these push-pull systems to evaluate the effect of TCBD entities in promoting charge polarization in the ground state and excited state charge transfer, and the role of PTZ in stabilizing the charge transfer states. The strong push-pull effects promoted charge polarization resulting in the extension of the absorption covering the 300-800 nm range. Electrochemical studies revealed electron exchange resulting in the splitting of the first reduction wave of TCBD in compounds C3, C4, 3, and 4 carrying two or three TCBD or PTZ-TCBD entities. Frontier orbitals on energy-optimized structures helped in arriving at different charge-transfer states. The spectrum of the charge transfer state was possible to arrive from spectroelectrochemical data. Finally, using pump-probe spectroscopy followed by Global target analysis, it has been possible to demonstrate the occurrence of excited charge transfer in these compounds, when the samples were excited both at the locally excited and charge polarized absorption peak maxima. The significance of the additional electron donor in these multi-modular systems in prolonging the lifetime of the charge transfer is borne out from the present study.

ASSOCIATED CONTENT

Supporting Information

¹H and ¹³C NMR, and MALDI-mass of synthesized compounds. Additional DPVs, CVs, spectroelectrochemical, and fs-TA spectral data.

AUTHOR INFORMATION

Corresponding Authors

Rajneesh Misra

Department of Chemistry, Indian Institute of Technology, Indore 453552, India; orcid.org/0000-0003-3225-2125; Email: rajneeshmisra@iiti.ac.in

Francis D'Souza

Department of Chemistry, University of North Texas, 1155 Union Circle, #305070, Denton, TX 76203-5017, USA, orcid.org/0000-0003-3815-8949, E-mail: Francis.DSouza@UNT.edu

Authors

Indresh Singh Yadav

Department of Chemistry, Indian Institute of Technology, Indore 453552, India

Ajyal Z. Alsaleh

Department of Chemistry, University of North Texas, 1155 Union Circle, #305070, Denton, TX 76203-5017, USA

Author Contributions

[‡]ISY and AZA contributed equally.

Notes

The authors declare no competing financial interest.

Acknowledgments

This research was supported by the US-National Science Foundation (2000988 to FD), Council of Scientific and Industrial Research (Project No. CSIR 01(2934)/18/EMR-II), New Delhi, and SERB (Project No. CRG/2018/000032) New Delhi, Govt. of India. We gratefully acknowledge the Sophisticated Instrumentation Centre (SIC), IIT Indore. IY is thankful to CSIR, India for a research fellowship.

References

- (1) Armaroli, N.; Balzani, V. The Future of Energy Supply: Challenges and Opportunities. *Angew. Chem. Int. Ed.* **2007**, *46* (1–2), 52–66.
- (2) Beaujuge, P. M.; Fréchet, J. M. J. Molecular Design and Ordering Effects in π -Functional Materials for Transistor and Solar Cell Applications. *J. Am. Chem. Soc.* **2011**, *133* (50), 20009–20029.
- (3) D'Souza, F.; Ito, O. Photosensitized Electron Transfer Processes of Nanocarbons Applicable to Solar Cells. *Chem. Soc. Rev.* **2011**, *41* (1), 86–96.
- (4) El-Khouly, M. E.; Fukuzumi, S.; D'Souza, F. Photosynthetic Antenna–Reaction Center Mimicry by Using Boron Dipyrromethene Sensitizers. *ChemPhysChem* **2014**, *15* (1), 30–47.
- (5) Bottari, G.; Torres, T. *Organic Nanomaterials: Synthesis, Characterization, and Device Applications,* Eds: Torres, T.; Bottari, G. John Wiley & Sons, Inc., Hoboken, NJ, **2013**.
- (6) Imahori, H.; Umeyama, T.; Ito, S. Large π -Aromatic Molecules as Potential Sensitizers for Highly Efficient Dye-Sensitized Solar Cells. *Acc. Chem. Res.* **2009**, *42* (11), 1809–1818.
- (7) Gust, D.; Moore, T. A.; Moore, A. L. Realizing Artificial Photosynthesis. *Faraday Discuss.* **2012**, *155* (0), 9–26.
- (8) Martín, N.; Sánchez, L.; Herranz, M. Á.; Illescas, B.; Guldi, D. M. Electronic Communication in Tetrathiafulvalene (TTF)/ C_{60} Systems: Toward Molecular Solar Energy Conversion Materials? *Acc. Chem. Res.* **2007**, *40* (10), 1015–1024.
- (9) Bottari, G.; de la Torre, G.; Guldi, D. M.; Torres, T. Covalent and Noncovalent Phthalocyanine–Carbon Nanostructure Systems: Synthesis, Photoinduced Electron Transfer, and Application to Molecular Photovoltaics. *Chem. Rev.* **2010**, *110* (11), 6768–6816.
- (10) Zarrabi, N.; Seetharaman, S.; Chaudhuri, S.; Holzer, N.; Batista, V. S.; van der Est, A.; D'Souza, F.; Poddutoori, P. K. Decelerating Charge Recombination Using Fluorinated Porphyrins in *N,N* -Bis(3,4,5-Trimethoxyphenyl)Aniline—Aluminum(III) Porphyrin—Fullerene Reaction Center Models. *J. Am. Chem. Soc.* **2020**, *142* (22), 10008–10024.
- (11) Hammarström, L. Accumulative Charge Separation for Solar Fuels Production: Coupling Light-Induced Single Electron Transfer to Multielectron Catalysis. *Acc. Chem. Res.* **2015**, *48* (3), 840–850.
- (12) Arrigo, A.; Santoro, A.; Puntoriero, F.; Lainé, P. P.; Campagna, S. Photoinduced Electron Transfer in Donor–Bridge–Acceptor Assemblies: The Case of Os(II)-Bis(Terpyridine)-(Bi)Pyridinium Dyads. *Coord. Chem. Rev.* **2015**, *304–305*, 109–116.
- (13) Fukuzumi, S.; Ohkubo, K.; Suenobu, T. Long-Lived Charge Separation and Applications in Artificial Photosynthesis. *Acc. Chem. Res.* **2014**, *47* (5), 1455–1464.

- (14) Gust, D.; Moore, T. A.; Moore, A. L. Solar Fuels via Artificial Photosynthesis. *Acc. Chem. Res.* **2009**, 42 (12), 1890–1898.
- (15) D'Souza, F.; Ito, O. Photosensitized Electron Transfer Processes of Nanocarbons Applicable to Solar Cells. *Chem. Soc. Rev.* **2011**, *41* (1), 86–96.
- (16) Barrejón, M.; Arellano, L. M.; D'Souza, F.; Langa, F. Bidirectional Charge-Transfer Behavior in Carbon-Based Hybrid Nanomaterials. *Nanoscale* **2019**, *11* (32), 14978–14992.
- (17) KC, C. B.; D'Souza, F. Design and Photochemical Study of Supramolecular Donor–Acceptor Systems Assembled via Metal–Ligand Axial Coordination. *Coord. Chem. Rev.* **2016**, *322*, 104–141.
 - (18) D. Kim, Multiporphyrin arrays: Fundamentals and applications, 2012.
- (19) Canton-Vitoria, R.; Gobeze, H. B.; Blas-Ferrando, V. M.; Ortiz, J.; Jang, Y.; Fernández-Lázaro, F.; Sastre-Santos, Á.; Nakanishi, Y.; Shinohara, H.; D'Souza, F.; Tagmatarchis, N. Excited-State Charge Transfer in Covalently Functionalized MoS2 with a Zinc Phthalocyanine Donor–Acceptor Hybrid. *Angew. Chem. Int. Ed.* **2019**, *58* (17), 5712–5717.
- (20) Misra, R.; Bhattacharyya, S. P. Nonlinear Optical Response of ICT Molecules. *Intramolecular Charge Transfer: Theory and Applications* **2018**.
- (21) May, V.; Kühn, O. *Charge and energy transfer dynamics in molecular systems*, John Wiley & Sons **2008**.
- (22) Gangala, S.; Misra, R. Spiro-Linked Organic Small Molecules as Hole-Transport Materials for Perovskite Solar Cells. *J. Mater. Chem. A* **2018**, *6* (39), 18750–18765.
- (23) Hagfeldt, A.; Boschloo, G.; Sun, L.; Kloo, L.; Pettersson, H. Dye-Sensitized Solar Cells. *Chem. Rev.* **2010**, *110* (11), 6595–6663.
- (24) Sun, L.; Bai, F.-Q.; Zhao, Z.-X.; Zhang, H.-X. Design of New Benzothiadiazole-Based Linear and Star Molecules with Different Functional Groups as Solar Cells Materials: A Theoretical Approach. *Solar Energy Materials and Solar Cells* **2011**, *95* (7), 1800–1810.
- (25) Rout, Y.; Gautam, P.; Misra, R. Unsymmetrical and Symmetrical Push–Pull Phenothiazines. *J. Org. Chem.* **2017**, *82* (13), 6840–6845.
- (26) Wu, Y.; Zhu, W. Organic Sensitizers from D $-\pi$ A to D-A- π A: Effect of the Internal Electron-Withdrawing Units on Molecular Absorption, Energy Levels and Photovoltaic Performances. *Chem. Soc. Rev.* **2013**, *42* (5), 2039–2058.
- (27) Berezin, M. Y.; Achilefu, S. Fluorescence Lifetime Measurements and Biological Imaging. *Chem. Rev.* **2010**, *110* (5), 2641–2684.
 - (28) Kivala, M.; Boudon, C.; Gisselbrecht, J.-P.; Seiler, P.; Gross, M.; Diederich, F. Charge-Transfer

- Chromophores by Cycloaddition–Retro-Electrocyclization: Multivalent Systems and Cascade Reactions. *Angew. Chem. Int. Ed.* **2007**, *46* (33), 6357–6360.
- (29) Bureš, F. Fundamental Aspects of Property Tuning in Push–Pull Molecules. *RSC Adv.* **2014**, *4* (102), 58826–58851.
- (30) Sailer, M.; Gropeanu, R.-A.; Müller, T. J. J. Practical Synthesis of Iodo Phenothiazines. A Facile Access to Electrophore Building Blocks. *J. Org. Chem.* **2003**, *68* (19), 7509–7512.
- (31) Franz, A. W.; Rominger, F.; Müller, T. J. J. Synthesis and Electronic Properties of Sterically Demanding N-Arylphenothiazines and Unexpected Buchwald–Hartwig Aminations. *J. Org. Chem.* **2008**, *73* (5), 1795–1802.
- (32) Peterson, B. M.; Ren, D.; Shen, L.; Wu, Y.-C. M.; Ulgut, B.; Coates, G. W.; Abruña, H. D.; Fors, B. P. Phenothiazine-Based Polymer Cathode Materials with Ultrahigh Power Densities for Lithium Ion Batteries. *ACS Appl. Energy Mater.* **2018**, *1* (8), 3560–3564.
- (33) Hart, A. S.; K. C., C. B.; Subbaiyan, N. K.; Karr, P. A.; D'Souza, F. Phenothiazine-Sensitized Organic Solar Cells: Effect of Dye Anchor Group Positioning on the Cell Performance. *ACS Appl. Mater. Interfaces* **2012**, *4* (11), 5813–5820.
- (34) Tancini, F.; Monti, F.; Howes, K.; Belbakra, A.; Listorti, A.; Schweizer, W. B.; Reutenauer, P.; Alonso-Gómez, J.-L.; Chiorboli, C.; Urner, L. M.; Gisselbrecht, J.-P.; Boudon, C.; Armaroli, N.; Diederich, F. Cyanobuta-1,3-Dienes as Novel Electron Acceptors for Photoactive Multicomponent Systems. *Chem. Eur. J.* **2014**, *20* (1), 202–216.
- (35) Gotfredsen, H.; Neumann, T.; Storm, F. E.; Muñoz, A. V.; Jevric, M.; Hammerich, O.; Mikkelsen, K. V.; Freitag, M.; Boschloo, G.; Nielsen, M. B. Donor–Acceptor-Functionalized Subphthalocyanines for Dye-Sensitized Solar Cells. *ChemPhotoChem* **2018**, *2* (11), 976–985.
- (36) Michinobu, T.; Diederich, F. The [2+2] Cycloaddition-Retroelectrocyclization (CA-RE) Click Reaction: Facile Access to Molecular and Polymeric Push-Pull Chromophores. *Angew. Chem. Int. Ed.* **2018**, *57* (14), 3552–3577.
- (37) Philippe, C.; Bui, A. T.; Beau, M.; Bloux, H.; Riobé, F.; Mongin, O.; Roisnel, T.; Cordier, M.; Paul, F.; Lemiègre, L.; Trolez, Y. Synthesis and Photophysical Properties of 1,1,4,4-Tetracyanobutadienes Derived from Ynamides Bearing Fluorophores. *Chem. Eur. J.* **2022**, *28* (23), e202200025.
- (38) Philippe, C.; Coste, M.; Bretonnière, Y.; Lemiègre, L.; Ulrich, S.; Trolez, Y. Quadruple Functionalization of a Tetraphenylethylene Aromatic Scaffold with Ynamides or Tetracyanobutadienes: Synthesis and Optical Properties. *Eur. J. Org. Chem.* **2022**, e202200049.
 - (39) Bui, A. T.; Philippe, C.; Beau, M.; Richy, N.; Cordier, M.; Roisnel, T.; Lemiègre, L.; Mongin, O.; Paul,

- F.; Trolez, Y. Synthesis, Characterization and Unusual near-Infrared Luminescence of 1,1,4,4-Tetracyanobutadiene Derivatives. *Chem. Commun.* **2020**, *56* (24), 3571–3574.
- (40) Pokladek, Z.; Ripoche, N.; Betou, M.; Trolez, Y.; Mongin, O.; Olesiak-Banska, J.; Matczyszyn, K.; Samoc, M.; Humphrey, M. G.; Blanchard-Desce, M.; Paul, F. Linear Optical and Third-Order Nonlinear Optical Properties of Some Fluorenyl- and Triarylamine-Containing Tetracyanobutadiene Derivatives. *Chem. Eur. J.* **2016**, *22* (29), 10155–10167.
- (41) Gopinath, A.; Manivannan, N.; Mandal, S.; Mathivanan, N.; Nasar, A. S. Substituent Enhanced Fluorescence Properties of Star α -Cyanostilbenes and Their Application in Bioimaging. *J. Mater. Chem. B* **2019**, *7* (39), 6010–6023.
- (42) Kivala, M.; Boudon, C.; Gisselbrecht, J.-P.; Seiler, P.; Gross, M.; Diederich, F. Charge-Transfer Chromophores by Cycloaddition–Retro-Electrocyclization: Multivalent Systems and Cascade Reactions. *Angew. Chem. Int. Ed.* **2007**, *46* (33), 6357–6360.
- (43) Sekita, M.; Ballesteros, B.; Diederich, F.; Guldi, D. M.; Bottari, G.; Torres, T. Intense Ground-State Charge-Transfer Interactions in Low-Bandgap, Panchromatic Phthalocyanine–Tetracyanobuta-1,3-Diene Conjugates. *Angew. Chem.* **2016**, *128* (18), 5650–5654.
- (44) Shoji, T.; Ito, S. Azulene-Based Donor–Acceptor Systems: Synthesis, Optical, and Electrochemical Properties. *Chem. Eur. J.* **2017**, *23* (66), 16696–16709.
- (45) Simón Marqués, P.; Castán, J. M. A.; Raul, B. A. L.; Londi, G.; Ramirez, I.; Pshenichnikov, M. S.; Beljonne, D.; Walzer, K.; Blais, M.; Allain, M.; Cabanetos, C.; Blanchard, P. Triphenylamine/Tetracyanobutadiene-Based π-Conjugated Push–Pull Molecules End-Capped with Arene Platforms: Synthesis, Photophysics, and Photovoltaic Response. *Chem. Eur. J.* **2020**, *26* (69), 16422–16433.
- (46) Winterfeld, K. A.; Lavarda, G.; Guilleme, J.; Sekita, M.; Guldi, D. M.; Torres, T.; Bottari, G. Subphthalocyanines Axially Substituted with a Tetracyanobuta-1,3-Diene–Aniline Moiety: Synthesis, Structure, and Physicochemical Properties. *J. Am. Chem. Soc.* **2017**, *139* (15), 5520–5529.
- (47) Winterfeld, K. A.; Lavarda, G.; Guilleme, J.; Guldi, D. M.; Torres, T.; Bottari, G. Subphthalocyanine–Tetracyanobuta-1,3-Diene–Aniline Conjugates: Stereoisomerism and Photophysical Properties. *Chem. Sci.* **2019**, *10* (48), 10997–11005.
- (48) Bui, A. T.; Philippe, C.; Beau, M.; Richy, N.; Cordier, M.; Roisnel, T.; Lemiègre, L.; Mongin, O.; Paul, F.; Trolez, Y. Synthesis, Characterization and Unusual near-Infrared Luminescence of 1,1,4,4-Tetracyanobutadiene Derivatives. *Chem. Commun.* **2020**, *56* (24), 3571–3574.
- (49) Gotfredsen, H.; Neumann, T.; Storm, F. E.; Muñoz, A. V.; Jevric, M.; Hammerich, O.; Mikkelsen, K. V.; Freitag, M.; Boschloo, G.; Nielsen, M. B. Donor–Acceptor-Functionalized Subphthalocyanines for Dye-

- Sensitized Solar Cells. ChemPhotoChem 2018, 2 (11), 976-985.
- (50) Gotfredsen, H.; Neumann, T.; Storm, F. E.; Muñoz, A. V.; Jevric, M.; Hammerich, O.; Mikkelsen, K. V.; Freitag, M.; Boschloo, G.; Nielsen, M. B. Donor–Acceptor-Functionalized Subphthalocyanines for Dye-Sensitized Solar Cells. *ChemPhotoChem* **2018**, *2* (11), 976–985.
- (51) Gautam, P.; Misra, R.; Thomas, M. B.; D'Souza, F. Ultrafast Charge-Separation in Triphenylamine-BODIPY-Derived Triads Carrying Centrally Positioned, Highly Electron-Deficient, Dicyanoquinodimethane or Tetracyanobutadiene Electron-Acceptors. *Chem. Eur. J.* **2017**, *23* (38), 9192–9200.
- (52) Sharma, R.; Thomas, M. B.; Misra, R.; D'Souza, F. Strong Ground- and Excited-State Charge Transfer in C3-Symmetric Truxene-Derived Phenothiazine-Tetracyanobutadine and Expanded Conjugates. *Angew. Chem.* **2019**, *131* (13), 4394–4399.
- (53) Rout, Y.; Jang, Y.; Gobeze, H. B.; Misra, R.; D'Souza, F. Conversion of Large-Bandgap Triphenylamine—Benzothiadiazole to Low-Bandgap, Wide-Band Capturing Donor—Acceptor Systems by Tetracyanobutadiene and/or Dicyanoquinodimethane Insertion for Ultrafast Charge Separation. *J. Phys. Chem. C* **2019**, *123* (38), 23382–23389.
- (54) Poddar, M.; Jang, Y.; Misra, R.; D'Souza, F. Excited-State Electron Transfer in 1,1,4,4-Tetracyanobuta-1,3-Diene (TCBD)- and Cyclohexa-2,5-Diene-1,4-Diylidene-Expanded TCBD-Substituted BODIPY-Phenothiazine Donor–Acceptor Conjugates. *Chem. Eur. J.* **2020**, *26* (30), 6869–6878.
- (55) Pinjari, D.; Alsaleh, A. Z.; Patil, Y.; Misra, R.; D'Souza, F. Interfacing High-Energy Charge-Transfer States to a Near-IR Sensitizer for Efficient Electron Transfer upon Near-IR Irradiation. *Angew. Chem. Int. Ed.* **2020**, *59* (52), 23697–23705.
- (56) Yadav, I. S.; Alsaleh, A. Z.; Misra, R.; D'Souza, F. Charge Stabilization via Electron Exchange: Excited Charge Separation in Symmetric, Central Triphenylamine Derived, Dimethylaminophenyl—Tetracyanobutadiene Donor—Acceptor Conjugates. *Chem. Sci.* **2021**, *12* (3), 1109–1120.
- (57) Jang, Y.; Rout, Y.; Misra, R.; D'Souza, F. Symmetric and Asymmetric Push–Pull Conjugates: Significance of Pull Group Strength on Charge Transfer and Separation. *J. Phys. Chem. B* **2021**, *125* (16), 4067–4075.
- (58) Khan, F.; Jang, Y.; Patil, Y.; Misra, R.; D'Souza, F. Photoinduced Charge Separation Prompted Intervalence Charge Transfer in a Bis(Thienyl)Diketopyrrolopyrrole Bridged Donor-TCBD Push-Pull System. *Angew. Chem. Int. Ed.* **2021**, *60* (37), 20518–20527.
- (59) Shinde, J.; Thomas, M. B.; Poddar, M.; Misra, R.; D'Souza, F. Does Location of BF2-Chelated Dipyrromethene (BODIPY) Ring Functionalization Affect Spectral and Electron Transfer Properties? Studies on α -, β -, and Meso-Functionalized BODIPY-Derived Donor–Acceptor Dyads and Triads. *J. Phys. Chem. C*

- **2021**, 125 (43), 23911–23921.
- (60) Sekaran, B.; Dawson, A.; Jang, Y.; MohanSingh, K. V.; Misra, R.; D'Souza, F. Charge-Transfer in Panchromatic Porphyrin-Tetracyanobuta-1,3-Diene-Donor Conjugates: Switching the Role of Porphyrin in the Charge Separation Process. *Chem. Eur. J.* **2021**, *27* (57), 14335–14344.
- (61) Yadav, I. S.; Jang, Y.; Rout, Y.; Thomas, M. B.; Misra, R.; D'Souza, F. Near-IR Intramolecular Charge Transfer in Strongly Interacting Diphenothiazene-TCBD and Diphenothiazene-DCNQ Push-Pull Triads. *Chem. Eur. J.* **2022**, *28* (25), e202200348.
- (62) Misra, R.; Maragani, R.; Gautam, P.; Mobin, S. M. Tetracyanoethylene Substituted Triphenylamine Analogues. *Tet. Letts.* **2014**, *55* (51), 7102–7105.
- (63) Frisch, M. J.; Trucks, G. W.; Schlegel, H. B.; Scuseria, G. E.; Robb, M. A.; Cheeseman, J. R.; Scalmani, G.; Barone, V.; Mennucci, B.; Petersson, G. A.; Nakatsuji, H.; Caricato, M.; Li, X.; Hratchian, H. P.; Izmaylov, A. F.; Bloino, J.; Zheng, G.; Sonnenberg, J. L.; Hada, M.; Ehara, M.; Toyota, K.; Fukuda, R.; Hasegawa, J.; Ishida, M.; Nakajima, T.; Honda, Y.; Kitao, O.; Nakai, H.; Vreven, T.; Montgomery, J. A., Jr.; Peralta, J. E.; Ogliaro, F.; Bearpark, M.; Heyd, J. J.; Brothers, E.; Kudin, K. N.; Staroverov, V. N.; Kobayashi, R.; Normand, J.; Raghavachari, K.; Rendell, A.; Burant, J. C.; Iyengar, S. S.; Tomasi, J.; Cossi, M.; Rega, N.; Millam, N. J.; Klene, M.; Knox, J. E.; Cross, J. B.; Bakken, V.; Adamo, C., Jaramillo, J.; Gomperts, R.; Stratmann, R. E.; Yazyev, O.; Austin, A. J.; Cammi, R.; Pomelli, C.; Ochterski, J. W.; Martin, R. L.; Morokuma, K.; Zakrzewski, V. G.; Voth, G. A.; Salvador, P.; Dannenberg, J. J.; Dapprich, S.; Daniels, A. D.; Farkas, O.; Foresman, J. B.; Ortiz, J. V.; Cioslowski, J.; Fox, D. J. Gaussian 09, Revision A.02; Gaussian, Inc., Wallingford, CT, 2009.
- (64) Rehm, D.; Weller, A. Kinetics of Fluorescence Quenching by Electron and H-Atom Transfer. *Isr. J. Chem.* **1970**, *8* (2), 259–271.
- (65) Snellenburg, J. J.; Laptenok, S.; Seger, R.; Mullen; K. M.; van Stokkum, I. H. Glotaran: A Java-based graphical user interface for the R package TIMP. *J. Stat. Softw.* **2012**, *49*, 1-22.
 - (66) http://glotaran.org/

TOC Graphic

